

RESEARCH ARTICLE | OCTOBER 30 2018

Transport and thermodynamic properties of the novel compound Nd₅CuSn₃

Special Collection: [21st International Conference on Magnetism](#)

Keisuke T. Matsumoto; Naoya Morioka; Koichi Hiraoka



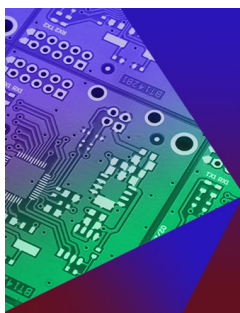
AIP Advances 8, 101341 (2018)

<https://doi.org/10.1063/1.5042435>View
OnlineExport
Citation

Articles You May Be Interested In

Magnetic phase transitions in R₅NiPb₃ (R = Ce, Nd, and Gd)*J. Appl. Phys.* (March 2009)Phase transitions in NdNiPb and Nd₅NiPb₃*J. Appl. Phys.* (January 2008)Low temperature crystal structure and magnetic properties of RAl₂*J. Appl. Phys.* (January 2014)

12 October 2024 23:21:29



AIP Electronic Devices

Fostering connections across multiple disciplines
in the broad electronics communityFollow us on  @aplecdevices AIP
Publishing[Learn More](#)

Transport and thermodynamic properties of the novel compound Nd_5CuSn_3

Keisuke T. Matsumoto,^a Naoya Morioka, and Koichi Hiraoka
*Graduate School of Science and Engineering, Ehime University, Matsuyama,
Ehime 790-8577, Japan*

(Received 31 May 2018; accepted 17 October 2018; published online 30 October 2018)

Electrical resistance R and specific heat C were measured to study the physical properties of the novel compound Nd_5CuSn_3 which crystallizes in the hexagonal Hf_5CuSn_3 -type structure. Nd ions occupy two non-equivalent sites. The values of R and C showed distinct anomalies at the magnetic transition temperature T_M of 56.3 K. The increments of T_M in the magnetic fields are consistent with the material being in a ferro- or ferri-magnetic state at temperatures below T_M . © 2018 Author(s). All article content, except where otherwise noted, is licensed under a Creative Commons Attribution (CC BY) license (<http://creativecommons.org/licenses/by/4.0/>). <https://doi.org/10.1063/1.5042435>

I. INTRODUCTION

Rare-earth-based intermetallic compounds exhibit various magnetic and electrical properties that arise from $4f$ electrons, such as magnetic ordering, higher-rank multipole ordering, and unconventional superconductivity.^{1–3} Ternary intermetallic compounds R_5TX_3 ($\text{R}=\text{Ce}, \text{Yb}, \text{T}=\text{Cu}, \text{Ag}, \text{X}=\text{Sn}, \text{Pb}$) have been observed to crystallize in the hexagonal Hf_5CuSn_3 -type structure.⁴ In this structure, rare-earth ions occupy two non-equivalent crystallographic sites: R1 ($4d$) and R2 ($6g$). The interatomic distance between R1 and R1 is shorter than that between R2 and R2 and that between R1 and R2. Ce_5CuSn_3 exhibits an antiferromagnetic transition at 3.5 K and heavy-fermion behavior with the Sommerfeld coefficient γ of 270 $\text{mJ/K}^2 \text{ mol Ce}$.⁵ For the La counterpart, the data for specific heat are explained as a combination of the Einstein and the Debye models.⁶ Isostructural heavy-fermion antiferromagnets Ce_5CuX_3 ($\text{X}=\text{Pb}, \text{Bi}$) have also been reported.⁷ Ce_5AgSn_3 orders ferromagnetically below 5 K.⁸ With the exception of Ce-based compounds, magnetic properties of Dy_5CuPb_3 , Gd_5NiPb_3 , and Nd_5NiPb_3 have also been studied.^{9–11} Dy_5CuPb_3 undergoes the two successive transitions: ferrimagnetic order at 45 K and antiferromagnetic order at 6.5 K. Gd_5NiPb_3 is ferrimagnetic below 68 K. Nd_5NiPb_3 shows antiferromagnetic order at 42 K and undergoes a weak-ferromagnetic spin canting transition at 8 K. These complex magnetic phase transitions are related to the two non-equivalent rare-earth ion sites in the crystal structure of each compound.

To the best of our knowledge, physical properties of R_5CuSn_3 compounds have not been studied, except for Ce_5CuSn_3 . In this study, we have carried out the measurements of the electrical resistance and specific heat of a polycrystalline sample of hexagonal Nd_5CuSn_3 . The results show that the compound underwent a phase transition at 56.3 K and suggest that this transition is of ferromagnetic or ferrimagnetic ordering.

II. EXPERIMENTAL PROCEDURE

A polycrystalline sample of Nd_5CuSn_3 was prepared by arc-melting stoichiometric amounts of the constituent elements (purity exceeding 99.9%) under an argon atmosphere. The sample was remelted several times to ensure homogeneity and was then annealed in an evacuated quartz ampule

^amatsumoto.keisuke.cv@ehime-u.ac.jp

at 600 °C for 1 week. It is worth noting that the Nd_5CuSn_3 compound easily oxidizes in air. Powder X-ray diffraction (XRD) patterns of the sample were carried out using a PANalytical X'Pert PRO with $\text{CuK}\alpha$ radiation. The standard four-probe method was used to measure the electrical resistance from 2 K to 300 K using a Physical Property Measurement System (PPMS, Quantum Design). Au wires were used for voltage and current leads and were attached using silver paste. Specific heat was measured using the PPMS in a temperature range of $2 \leq T \leq 200$ K under an applied magnetic field of up to 7 T.

III. RESULTS AND DISCUSSION

Figure 1 presents the XRD patterns of Nd_5CuSn_3 . The diffraction peaks indicate that the hexagonal Hf_5CuSn_3 -type structure is the primary phase. The impurity phase may be associated with Cu_2O . The estimated lattice constants are $a=9.348$ Å and $c=6.684$ Å, which are smaller than those of Ce_5CuSn_3 . These values agree with the trend expected from the lanthanide contraction.

Figure 2 shows the temperature dependence of the electrical resistance R , normalized to the value at 300 K for Nd_5CuSn_3 . Owing to micro-cracks in this sample, the geometric dimensions could not be determined exactly. This cracking phenomenon has been observed in other R_5TX_3 samples, such

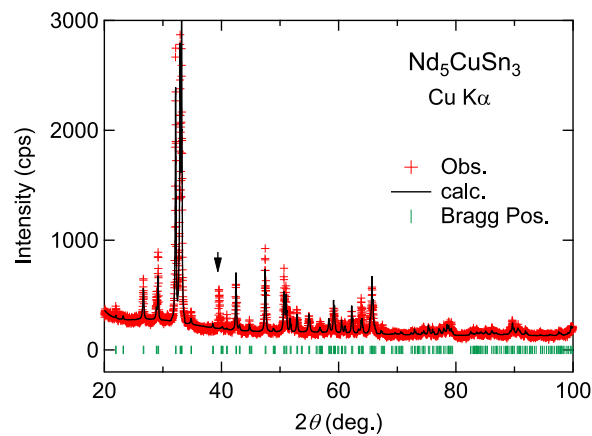


FIG. 1. Powder X-ray diffraction pattern of Nd_5CuSn_3 . The solid lines are calculated profile obtained by the Rietveld refinement using a program RIETAN-FP.¹⁷ The vertical lines mark the positions of possible Bragg reflections. The black arrow indicates the peak of the impurity phase.

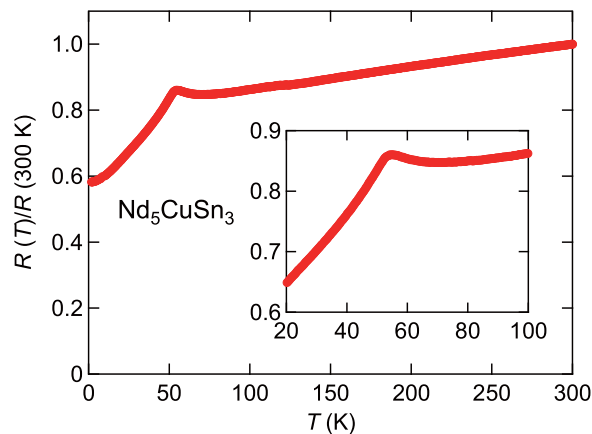


FIG. 2. Electrical resistance normalized to the value at 300 K as a function of temperature for Nd_5CuSn_3 . The inset is an enlargement of the resistance around 60 K.

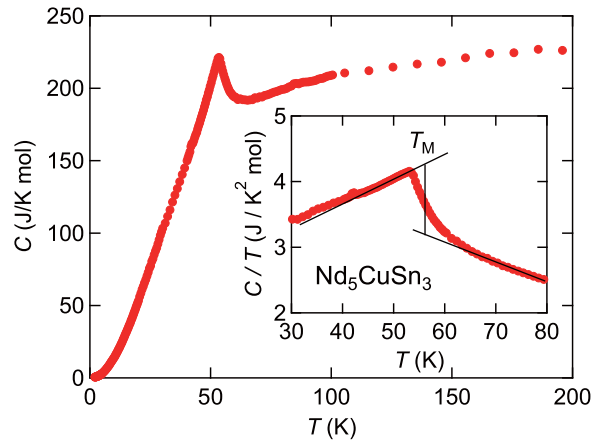


FIG. 3. Temperature dependence of the specific heat C at zero field of Nd_5CuSn_3 . The inset shows C/T versus T near the magnetic transition temperature.

as Ce_5CuSn_3 ,⁵ Ce_5CuPb_3 ,⁶ and Dy_5CuPb_3 .⁹ R depended only weakly on temperature above 100 K and featured a shoulder at around 60 K, as shown in the inset of Fig. 2. This shoulder indicates a phase transition. A similar maximum in the $R(T)$ curve has been reported for RNi_5 ¹² and Dy_5CuPb_3 .⁹ This cusp-like anomaly may be attributed to the scattering caused by critical fluctuations above the phase-transition temperature. Below T_M , $R(T)$ decreased with decreasing temperature due to the reduction in spin-disorder scattering in the magnetically ordered state.

The data of specific heat C for Nd_5CuSn_3 in zero magnetic field are plotted against temperature in Fig. 3. At 200 K, C reached approximately 225 J/K mol, which is close to the Dulong-Petit value of 221 J/K mol. A clear jump in $C(T)$ appeared at around 55 K as observed from $R(T)$ measurement, indicating the bulk nature of the phase transition. The magnetic transition temperature T_M is 56.3 K, as determined from the midpoint of the jump in the C/T curve, which is shown in the inset of Fig. 3. All data for $C(T)$ in magnetic fields up to 7 T are plotted in Fig. 4. The temperatures at which C showed a peak were shifted to higher temperatures and the peak broadened with increasing magnetic field. This result suggests that this transition is ferromagnetic or ferrimagnetic ordering at T_M . In case of a ferromagnetic metal with a non-cubic crystal structure, C below T_M is expected to obey the following equation;

$$C = \gamma T + \beta T^3 + \alpha T^{3/2} e^{-\Delta/T}, \quad (1)$$

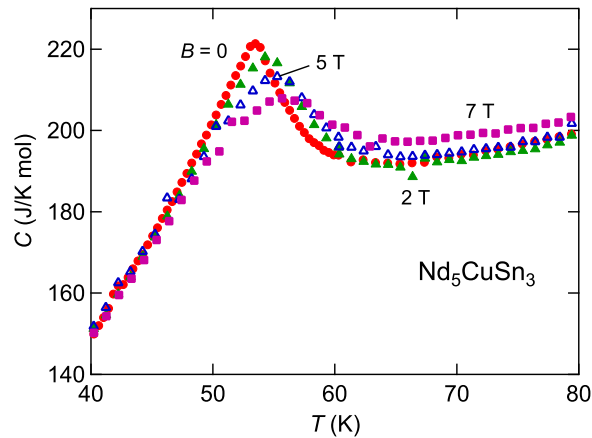


FIG. 4. Temperature dependence of specific heat at various magnetic fields of 0 T (red closed circles), 2 T (green closed triangles), 5 T (open triangles), and 7 T (purple closed squares).

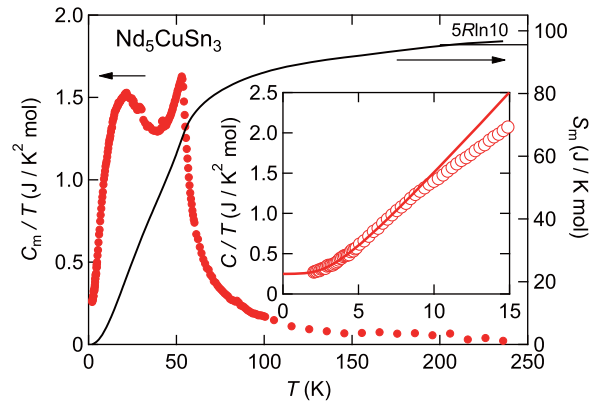


FIG. 5. Temperature dependences of the magnetic specific heat divided by temperature (left-hand scale) and the magnetic entropy (right-hand scale). The inset shows the low temperature part of C/T versus T for Nd_5CuSn_3 . The solid line represents a fit according to Eq. (1).

where the first term represents the electronic contribution, the second represents a low temperature approximation of the lattice contribution, and the third term represents the conventional form of a magnon contribution (α , β , and γ are constants and Δ represents the magnon gap).¹⁵ The least-squares fit of the formula to the experimental results below 8 K (shown in the inset of Fig. 5) yields the following parameters: the Sommerfeld coefficient $\gamma \sim 250 \text{ mJ/K}^2 \text{ mol}$ ($50 \text{ mJ/K}^2 \text{ mol Nd}$), $\beta \sim 3 \text{ mJ/K}^4 \text{ mol}$, $\alpha \sim 0.75 \text{ J/K}^{2.5} \text{ mol}$, and $\Delta \sim 9 \text{ K}$. The Sommerfeld coefficient for Nd_5CuSn_3 is $50 \text{ mJ/K}^2 \text{ mol Nd}$, which is 10 times larger than that for La_5CuSn_3 of $4.5 \text{ mJ/K}^2 \text{ mol La}$ ⁵ and is 5 times larger than those of other Nd-based compounds: $5 \text{ mJ/K}^2 \text{ mol Nd}$ for Nd_2Al ¹³ and $9.5 \text{ mJ/K}^2 \text{ mol}$ for NdAl_2 .¹⁴ The Debye temperature of the sample is estimated to be 180 K, assuming nine Debye oscillators. The magnetic specific heat C_m is estimated by subtracting the Debye specific heat C_D from the measured data. The equation for C_D is represented as

$$C_D = 9nN_A k_B \left(\frac{T}{\Theta_D} \right)^3 \int_0^{\Theta_D/T} \frac{x^4 e^x}{(e^x - 1)^2} dx, \quad (2)$$

where n is the number of the Debye oscillators, N_A is the Avogadro's number, and k_B is the Boltzmann constant. Here we use $\Theta_D = 180 \text{ K}$ obtained by the fitting of Eq. (1). The calculated values for C_m/T and S_m are plotted in Fig. 5. S_m was calculated by integrating C_m/T with respect to temperature. S_m reaches $5R \ln 10$ around 250 K.

The analysis of the magnetic specific heat indicates that the electronic contribution is very small ($\gamma \sim 0$), whereas a large value of $\gamma = 50 \text{ mJ/K}^2 \text{ mol Nd}$ was obtained by the fitting the data at low temperatures. A large value of γ was also observed in the isostructural compound Nd_5NiPb_3 ¹¹ and was attributed to spin fluctuations arising from the two non-equivalent Nd sites. For Nd_5CuSn_3 , a peak in C_m/T at around 20 K, as shown in Fig. 5, may be attributed to the complex magnetic interaction originated from the two non-equivalent Nd sites. The large γ may also originate in the hybridization between f -electrons and conduction electrons. To estimate the value of A/γ^2 (Kadowaki-Woods relationship),¹⁶ where A is the coefficient of resistivity ρ expressed as $\rho \propto AT^2$, a large-grain specimen of Nd_5CuSn_3 will be needed to determine the absolute resistivity value. To study the magnetic ordering of this compound in more detail, magnetization measurements are now in progress.

IV. SUMMARY

We have prepared the novel Nd_5CuSn_3 compound which crystallizes in the hexagonal structure. Electrical resistance and specific heat measurements revealed that Nd_5CuSn_3 exhibited a phase transition at $T_M = 56.3 \text{ K}$. With increasing magnetic field, the peak in $C(T)$ broadened and appeared at higher temperatures. These results suggest that the transition at T_M indicates the formation of ferromagnetic or ferrimagnetic ordering in the sample.

ACKNOWLEDGMENTS

Electrical resistance and specific heat measurements were carried out at the Faculty of Science, Ehime University, Japan. KTM was financially supported by a tenure track program of Ehime University, Japan.

- ¹ F. R. de Boer, J. C. P. Klaasse, P. A. Veemhuizen, A. Bohm, C. D. Breidl, U. Gottwick, H. M. Mayer, L. Pawlak, U. Rauchschwalbe, H. Spille, and F. Steglich, *J. Mag. Mag. Mater.* **63**, 91 (1987).
- ² P. Morin, D. Schmitt, and E. du Tremolet de Lacheisserie, *J. Mag. Mag. Mater.* **30**, 257 (1982).
- ³ F. Steglich, J. Aarts, C. D. Breidl, W. Lieke, D. Meschede, W. Franz, and H. Schäfer, *Phys. Rev. Lett.* **43**, 1892 (1979).
- ⁴ W. Rieger and E. Parthé, *Monatshefte fuer Chemie* **99**, 291 (1968).
- ⁵ V. H. Tran, *J. Alloys and Comp.* **383**, 281 (2004).
- ⁶ V. H. Tran, *Czech. J. Phys.* **54**, D411 (2004).
- ⁷ V. H. Tran, M. Gamza, A. Ślebarski, W. Miiller, and J. Jarmulska, *J. Alloys and Comp.* **451**, 457 (2008).
- ⁸ P. Boulet, D. Mazzone, H. Noël, P. Riani, P. Rogl, and R. Ferro, *Intermetallics* **7**, 931 (1999).
- ⁹ V. H. Tran and L. D. Gulay, *J. Solid State Chem.* **179**, 646 (2006).
- ¹⁰ V. Goruganti, K. D. D. Rathnayaka, and J. H. Ross, Jr., *J. Appl. Phys.* **103**, 07B709 (2008).
- ¹¹ V. Goruganti, K. D. D. Rathnayaka, and J. H. Ross, Jr., *J. Appl. Phys.* **105**, 07E118 (2009).
- ¹² J. A. Blanco, D. Gignoux, D. Schmitt, A. Tari, and F. Y. Bang, *J. Phys.: Condens. Matter* **6**, 4335 (1994).
- ¹³ J. C. P. Campoy, E. J. R. Plaza, A. A. Coelho, and S. Gama, *Phys. Rev. B* **74**, 134410 (2006).
- ¹⁴ P. Kumar, K. G. Suresh, and A. K. Nigam, *J. Phys. D* **41**, 105007 (2008).
- ¹⁵ T. Fukuhara, R. Yamagata, L. Li, K. Nishimura, and K. Maezawa, *J. Phys. Soc. Jpn.* **78**, 034723 (2009).
- ¹⁶ K. Kadowaki and S. B. Woods, *Solid State. Commun.* **58**, 507 (1986).
- ¹⁷ F. Izumi and K. Momma, *Solid State Phenom* **130**, 15 (2007).